PHYSICAL REVIEW C **66**, 054006 (2002)

Elastic scattering of charged pions from ^{3}H and ^{3}He

W. J. Briscoe, B. L. Berman, R. W. C. Carter,* K. S. Dhuga, S. K. Matthews,† and N-J. Nicholas‡
Center for Nuclear Studies, Department of Physics, The George Washington University, Washington D.C. 20052

S. J. Greene
Los Alamos National Laboratory, Los Alamos, New Mexico 87545

B. M. K. Nefkens and J. W. Price
Department of Physics, University of California at Los Angeles, Los Angeles, California 90095

L. D. Isenhower and M. E. Sadler
Department of Physics, Abilene Christian University, Abilene, Texas 79699

I. Šlaus and I. Supek
Rudjer Bošković Institute, Zagreb, Croatia
(Received 22 April 2002; published 27 November 2002)

We have measured the ratios of normalized yields for the elastic scattering of charged pions from ^{3}H and ^{3}He in the backward hemisphere. At $T_\pi = 180$ MeV, we have completed the angular distribution measured earlier, adding six new data points in the angular range from 119° to 169° in the π-nucleus center of mass. We also measured an excitation function with data points at $T_\pi = 142$, 180, 220, and 256 MeV at the largest angle achievable with our detector—between 160° and 170° in the π-nucleus center of mass. The data, taken as a whole, show an apparent role reversal of the two charge-symmetric ratios r_1 and r_2 in the backward hemisphere. For data $\geqslant 100°$ we observe a strong dependence of the ratios on $-t$, independent of T_π or θ_π. The superratio R data match very well with calculations based on the forward-hemisphere data that predict the value of the difference between the even-nucleon radii of ^{3}H and ^{3}He. Comparisons are also made with recent calculations incorporating different wave functions and double-scattering models.

DOI: 10.1103/PhysRevC.66.054006 PACS number(s): 25.55.Ci, 25.80.Dj, 25.10.+s, 27.10.+h

I. INTRODUCTION

This is the final report of a series of experiments on tests of charge symmetry using π^+ and π^- elastic scattering on tritium and helium-3. The scientific motivation, experimental techniques, and details of our experimental apparatus, such as the pressurized gas targets including the tritium container for nearly 200 000 ci of tritium, are given in Refs. [1–6]. A detailed theoretical analysis is presented in a separate paper [7]. Below we review the basic parameters and final results of our experiment.

The first experimental parameters are the ratios r_1 and r_2:

$$r_1 = \frac{d\sigma(\pi^{+\,3}\mathrm{H})}{d\sigma(\pi^{-\,3}\mathrm{He})} \tag{1}$$

and

$$r_2 = \frac{d\sigma(\pi^{-\,3}\mathrm{H})}{d\sigma(\pi^{+\,3}\mathrm{He})}. \tag{2}$$

By charge symmetry these ratios should be equal to one at all energies and t values, where $-t$ is the four-momentum transfer squared. Since the form factor of ^{3}He is smaller than that of ^{3}H because of the Coulomb repulsion between the protons, the cross section in the denominator is reduced and we expect that the ratios r_1 and r_2 will be somewhat greater than one [8,9]. For r_1, scattering from the odd (unpaired) nucleon dominates in the Δ energy region, and so the scattering is a mixture of spin flip and nonspin flip. For r_2, scattering from the even (paired) nucleon dominates, and so spin-flip scattering is suppressed.

The next ratio is R, the "superratio." It is defined as the product of r_1 and r_2,

$$R = r_1 \cdot r_2. \tag{3}$$

By charge symmetry R must be one.

Finally, we define

$$\rho^+ = \frac{d\sigma(\pi^{+\,3}\mathrm{H})}{d\sigma(\pi^{+\,3}\mathrm{He})} \tag{4}$$

and

*Present address: 1627 Camden Ave., No. 307, Los Angeles, CA 90025.

†Present address: Oregon Hearing Research Center, Oregon Health Science University, Portland, OR 97201-3098.

‡Present address: Advanced Nuclear Technology Group (NIS-6), MS J562, Nonproliferation and International Security Division, LANL, Los Alamos, NM 87545.

TABLE I. Measured values of the ratios from this experiment. The quoted uncertainties are statistical only.

T_π (MeV)	$\theta^{(\circ)}$	$-t(\mathrm{fm}^{-2})$	ρ^+	ρ^-	r_1	r_2	R
142	160.0	5.0	0.811 (0.024)	1.347 (0.065)	1.10 (0.06)	0.99 (0.06)	1.09 (0.06)
142	163.6	5.0	0.757 (0.027)	1.401 (0.086)	1.08 (0.05)	1.01 (0.06)	1.09 (0.06)
180	119.4	5.2	0.85 (0.02)	1.28 (0.04)	1.07 (0.04)	1.02 (0.04)	1.09 (0.04)
180	129.8	5.7	0.87 (0.02)	1.38 (0.04)	1.13 (0.04)	1.06 (0.04)	1.20 (0.05)
180	139.1	6.1	0.75 (0.03)	1.56 (0.08)	1.15 (0.06)	1.01 (0.07)	1.16 (0.08)
180	148.3	6.4	0.55 (0.02)	2.05 (0.09)	1.09 (0.05)	1.03 (0.06)	1.13 (0.06)
180	157.4	6.7	0.44 (0.01)	2.62 (0.11)	1.08 (0.05)	1.06 (0.06)	1.14 (0.06)
180	169.2	6.9	0.38 (0.01)	3.06 (0.15)	1.12 (0.06)	1.05 (0.06)	1.18 (0.06)
220	169.3	8.9	0.408 (0.035)	2.86 (0.18)	1.21 (0.11)	0.97 (0.07)	1.17 (0.09)
256	169.4	10.9	0.478 (0.035)	2.59 (0.37)	1.25 (0.20)	0.99 (0.16)	1.24 (0.20)

$$\rho^- = \frac{d\sigma(\pi^{-3}\mathrm{H})}{d\sigma(\pi^{-3}\mathrm{He})}. \tag{5}$$

These ratios are not charge symmetric, but several experimental uncertainties cancel when calculating ρ^+ and ρ^-, and they can be used to derive the charge symmetric R with lower experimental uncertainty, since

$$R = \rho^+ \cdot \rho^-. \tag{6}$$

In Sec. II, we briefly discuss the analysis of our data at energies spanning the Δ_{33} resonance. The results are presented in Sec. III. In Sec. IV, we discuss the results for angles greater than 100°. Finally, we summarize our findings in Sec. V.

II. EXPERIMENT

The experimental details have been given by Matthews *et al.* [4]. Here, we briefly discuss the analysis of the data and the relevant experimental parameters for the determination of the scattering ratios.

The ratios r_1 and r_2 are extracted as

$$r_1 = \frac{Y(\pi^{+3}\mathrm{H})}{Y(\pi^{+2}\mathrm{H})} \cdot \frac{Y(\pi^{-2}\mathrm{H})}{Y(\pi^{-3}\mathrm{He})} \cdot \frac{d\sigma(\pi^{+2}\mathrm{H})}{d\sigma(\pi^{-2}\mathrm{H})} \cdot \frac{N_{3_{\mathrm{He}}}}{N_{3_{\mathrm{H}}}} \tag{7}$$

and

$$r_2 = \frac{Y(\pi^{-3}\mathrm{H})}{Y(\pi^{-2}\mathrm{H})} \cdot \frac{Y(\pi^{+2}\mathrm{H})}{Y(\pi^{+3}\mathrm{He})} \cdot \frac{d\sigma(\pi^{-2}\mathrm{H})}{d\sigma(\pi^{+2}\mathrm{H})} \cdot \frac{N_{3_{\mathrm{He}}}}{N_{3_{\mathrm{H}}}}, \tag{8}$$

where $Y(\pi^{\pm n}A)$ refers to the scattering yield, and $N_{3_{\mathrm{H}}}$ and N^3He are the number density of scattering centers in the ^{3}H and ^{3}He samples, respectively [4]. Elastic scattering yields from ^{2}H are used to scale the other yields to the known $\pi^{\pm 2}$H cross sections. Writing the ratio $d\sigma(\pi^{+2}\mathrm{H})/d\sigma(\pi^{-2}\mathrm{H})$ as D, and defining Y_N as the yield per target nucleon $Y(\pi^{\pm n}A/N_A)$, we have

$$r_1 = \frac{Y_N(\pi^{+3}\mathrm{H}) \cdot Y(\pi^{-2}\mathrm{H}) \cdot D}{Y_N(\pi^{-3}\mathrm{He}) \cdot Y(\pi^{+2}\mathrm{H})} \tag{9}$$

and similarly

$$r_2 = \frac{Y_N(\pi^{-3}\mathrm{H}) \cdot Y(\pi^{+2}\mathrm{H})}{Y_N(\pi^{+3}\mathrm{He}) \cdot Y(\pi^{-2}\mathrm{H}) \cdot D}. \tag{10}$$

Then

$$R = \frac{Y_N(\pi^{+3}\mathrm{H}) \cdot Y_N(\pi^{-3}\mathrm{H})}{Y_N(\pi^{-3}\mathrm{He}) \cdot Y_N(\pi^{+3}\mathrm{He})}. \tag{11}$$

In the definitions of r_1 and r_2, it is the *ratio* of the $\pi^{\pm 2}$H yields and cross sections that appears. All normalization quantities not related to $N_{3_{\mathrm{H}}}$ and $N_{3_{\mathrm{He}}}$ cancel in R.

Finally, we consider the ratios ρ^+ and ρ^-. Since the same charge of pion appears in both the numerator and denominator of each of these ratios, the non-target-related normalization quantities cancel here as well. Then we have

$$\rho^+ = \frac{Y_N(\pi^{+3}\mathrm{H})}{Y_N(\pi^{+3}\mathrm{He})} \tag{12}$$

and

$$\rho^- = \frac{Y_N(\pi^{-3}\mathrm{H})}{Y_N(\pi^{-3}\mathrm{He})}, \tag{13}$$

so that

$$R = r_1 \cdot r_2 = \rho^+ \cdot \rho^-. \tag{14}$$

III. RATIOS

Values for all of the ratios measured in this experiment are given in Table I. Figure 1 shows the angular distributions for the simple charge-symmetric ratios r_1 and r_2, as well as the superratio R at 142, 180, 220, and 256 MeV. To provide a useful overview, we have included our earlier data obtained

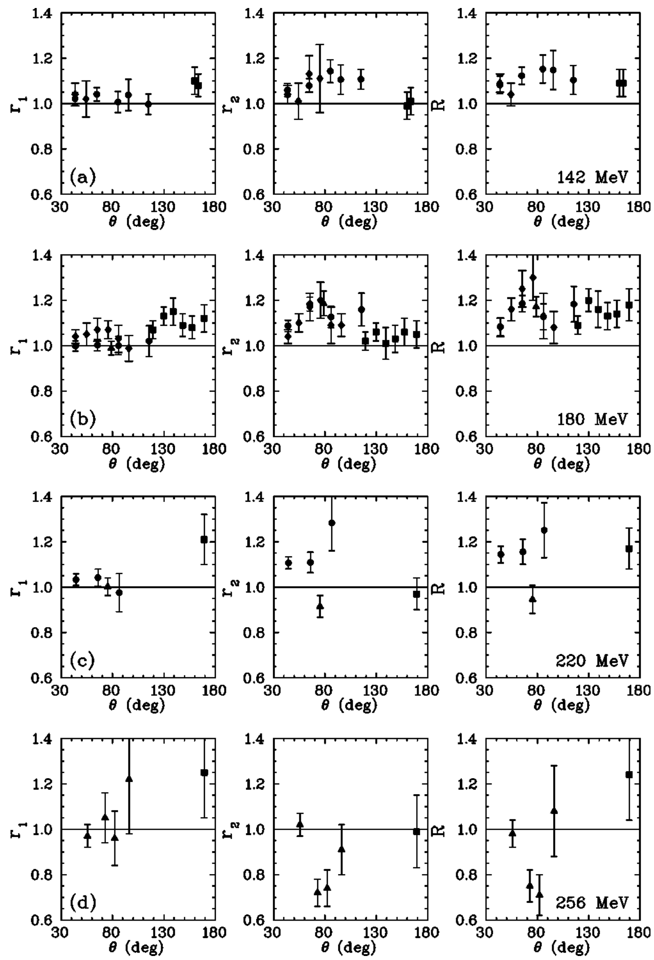

FIG. 1. The ratios r_1, r_2 and the superratio R for $\pi^{\pm}$ ^{3}H/^{3}He elastic scattering plotted versus the center-of-mass angle in the π-^3A system for various incident pion kinetic energies: (a) $T_\pi = 142$ MeV, (b) 180 MeV, (c) 220 MeV, and (d) 256 MeV. Experimental data are from Refs. [1] (diamonds), [2] (circles), and [6] (triangles), and this experiment (squares).

at forward angles. We see that r_1 is flat and structureless in the forward hemisphere but rises in the backward hemisphere where it remains high to about 170°. The ratio r_2 shows structure at about 80° in the forward hemisphere, approaches 1.0 in the backward hemisphere, and stays there to 170°. Most of the structure in R is therefore due to r_2.

We note that, aside from the region near 80° in the π-^3A center-of-mass kinematics, which corresponds to 90° in the π-N center of mass where the non-spin-flip scattering amplitudes have zeros, the charge-symmetric scattering ratios do not have any sharp features. Indeed, in the backward hemisphere they are fairly flat and quite smooth. This is not surprising, since the π-nucleon amplitudes are smooth and have no zeros in this region. The form factors for ^{3}H and ^{3}He, as measured with electron scattering, are smooth as well. Finally, the interactions in the numerator and denominator for each ratio are approximately the same: primarily odd nucleon in r_1, and primarily even nucleon in r_2. R is the smooth product of two smooth functions.

Of more interest is the general trend of the ratios as we

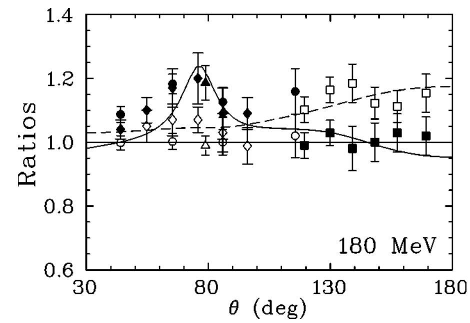

FIG. 2. The simple ratios r_1 (open symbols) and r_2 (filled symbols) are compared to the calculations of Ref. [7] for r_1 (dashed line) and r_2 (solid line). The qualitative behavior of the simple ratios, including the crossover, were first predicted by an optical-model calculation by Gibbs and Gibson (Ref. [10]) before the back-angle data were taken. We used the results of Smith *et al.* (Ref. [11]) which give a value of 1.03 for the ratio of the yield for $(\pi^{+2}\mathrm{H})/(\pi^{-2}\mathrm{H})$ at back angles. A slight improvement of χ^2 is obtained by using the value 1.03 over assuming that this ratio is equal to 1.00 as is required by charge symmetry and indicated by the SAID fit to the existing π-^{2}H data (Ref. [12]).

progress from the forward to the backward hemisphere as shown in Fig. 2. The crossover of the two ratios, and the fact that r_1 is significantly different from unity, are r_2 is consistent with unity is difficult to explain quantitatively. It is interesting to note that the qualitative behavior of the simple ratios, including the crossover, was first predicted in an optical-model calculation by Gibbs and Gibson [10] before the back-angle data were taken.

One might speculate that as one passes to the backward hemisphere, with the diminishing importance of the single-scattering process, the double-scattering process provides a mechanism for spin-flip amplitudes to contribute in paired-nucleon scattering without violating the Pauli exclusion principle. We refer the reader to the accompanying paper for a thorough discussion of this issue [7].

Figure 3 shows our results for ρ^+ and ρ^-. These ratios have very small error bars, owing to the cancellation of the normalization quantities mentioned above. The steep rise of ρ^- and the fall below one of ρ^+ at angles $\geqslant 100°$ are indications that there is a steep rise in the 180-MeV even-nucleon-dominated cross sections in the backward hemisphere [4]. The error bars for these ratios are much smaller than those for the cross sections and r_1 or r_2. Even though ρ^+ and ρ^- are not themselves charge symmetric, they provide a means of calculating R with minimum experimental uncertainty.

Figure 4 shows R at 180 MeV. The shape is derived from the two simple ratios, the bump at 80° corresponding to the bump in r_2 and the steady rise in the backward hemisphere to the rise in r_1. Figure 4 also shows the calculations by Kudryavtsev *et al.* [7] and by Gibbs and Gibson [10]. In the latter, the shape of the superratio was used to extract the difference in the odd- and even-nucleon radii more precisely than is possible from existing electron-scattering data. The optical-model calculation of Ref. [10] shows a strong dependence on two parameters, the difference between the rms

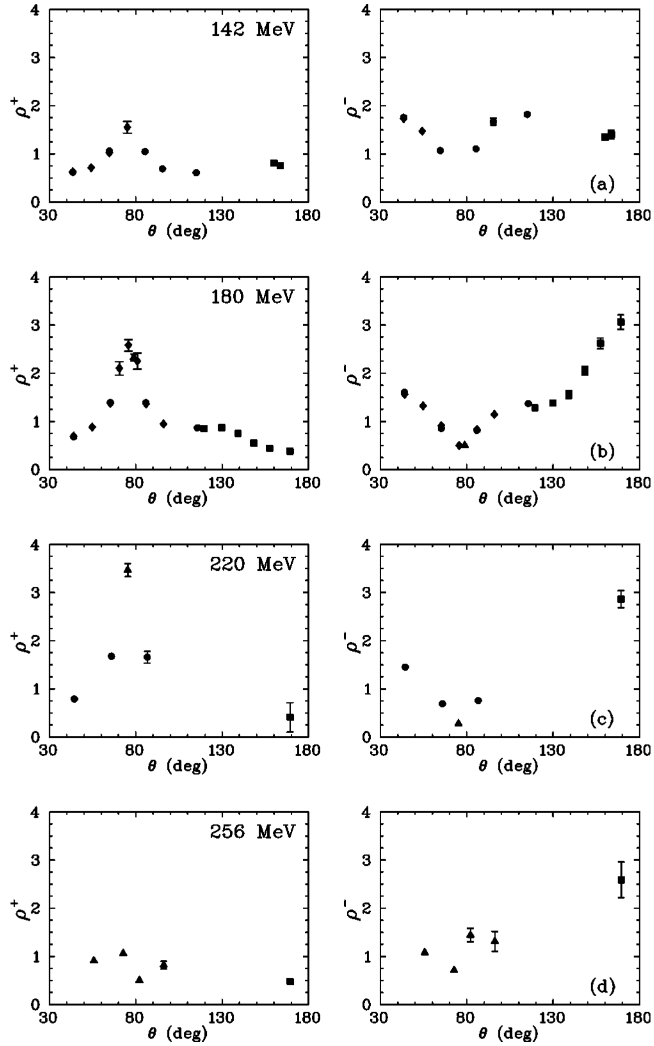

FIG. 3. The ratios ρ^+ and ρ^- for (a) T_π=142 MeV, (b) 180 MeV, (c) 220 MeV, and (d) 256 MeV. The notation for the experimental data is the same as for Fig. 1.

neutron radius in tritium and the rms proton radius in ^{3}He (that is, the difference in the even-nucleon radii), and the difference between the rms proton radius in ^{3}H and the rms neutron radius in ^{3}He. In the approach of Ref. [7], a successful description of R at T_π=180 MeV is based on the difference in the wave functions of ^{3}H and ^{3}He and on the Δ_{33} mass splitting as well as on the inclusion of the double-scattering interaction of the pion with nucleons of the target nuclei. Both models account for the role reversal of the r_1 and r_2 at back angles at T_π=180 MeV. However, Kudryavtsev *et al.* fitted r_1 and r_2 to determine R, while Gibbs and Gibson fitted their calculations to R and inferred r_1 and r_2 before the data were obtained.

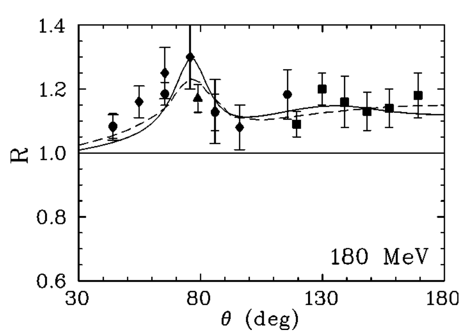

FIG. 4. The superratio R at T_π=180 MeV is compared to calculations by Kudryavtsev *et al.* (Ref. [7]) (solid curve) and Gibbs and Gibson (Ref. [10]) (dashed curve). The notation for the experimental data is the same as in Fig. 1.

Although the leading terms included in the calculation of Kudryavtsev *et al.* reproduce the main features of the back-angle ratios at energies of 180 MeV and above, another factor which might contribute to this remarkable role reversal of r_1 and r_2 at back angles is a two-step process consisting of the formation of a Δ by the interaction of the incident pion with a nucleon, followed by the scattering of this Δ on the remaining correlated nucleon pair. This process is clearly overshadowed by single scattering at angles near the non-spin-flip dip, but, like any two-step process, could become important as the momentum transfer increases.

For r_1, the dominant channels for Δ formation would be $\pi^+ + p \rightarrow \Delta^{++}$ in the numerator and $\pi^- + n \rightarrow \Delta^-$ in the denominator, whereas the reverse would be the case for r_2. [For r_1 the correlated pairs would be (nn) in the numerator and (pp) in the denominator, and for r_2 they would be (np) pairs in both numerator and denominator.] The width of the Δ^{++} is somewhat smaller than that of the Δ^- (about 5 MeV out of a total width of about 120 MeV [13]), and the lifetime of the former would be longer than that of the latter. In the framework of a multiple scattering picture, the ratios we measure are in effect, after other terms cancel, ratios of propagators and are sensitive to small differences in width. Thus, at back angles where multiple scattering becomes increasingly important, Δ mass and width differences may contribute to the observed effect of increasing r_1 and decreasing r_2.

IV. DEPENDENCE ON MOMENTUM TRANSFER

Figure 5 shows r_1, r_2, and R at the large scattering angles ($\geqslant 100°$) for all pion energies plotted versus the four-momentum transfer squared. In Fig. 5(a), r_1 increases steadily, while in Fig. 5(b), r_2 decreases slightly with $-t$. R displays a very slight increase with the four-momentum transfer squared, as shown in Fig. 5(c). From Fig. 5 one can conclude that, since r_1, r_2, and R, coming from different energy sets, fall on top of each other and follow the same general trend, these ratios are primarily functions of $-t$.

The behavior of ρ^+ and ρ^- at the largest scattering angles versus T_π can be observed with the help of Table I. As seen in the table, ρ^+ decreases sharply from 142 to 180 MeV, then rises slightly through 220 and 256 MeV. ρ^- shows the opposite behavior, with a maximum at 180 MeV. The excitation functions for ρ^+ and $1/\rho^-$ for backward angles versus $-t$ are shown in Fig. 6. As is the case for r_1, r_2, and R, the agreement of the overlaid data at different energies is also quite good.

We note that in the forward hemisphere, a model that assumes single π-N scattering explains the behavior of elas-

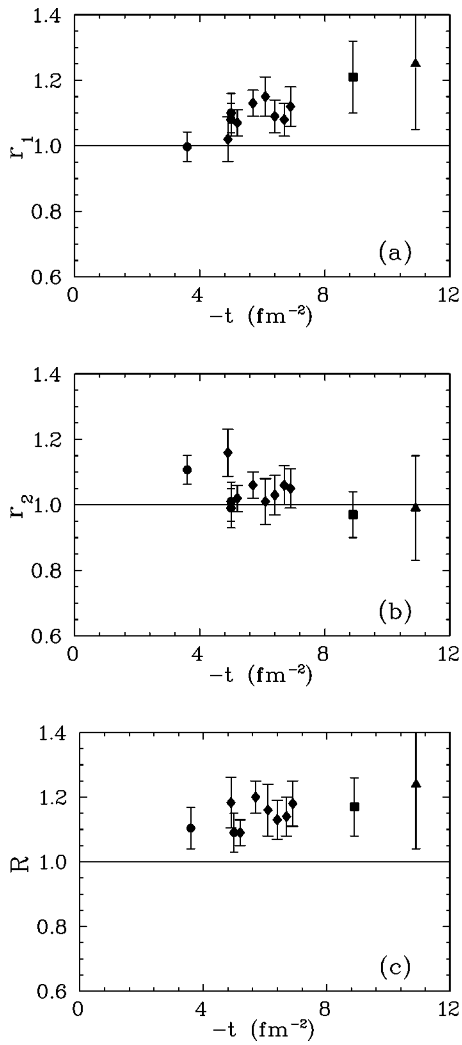

FIG. 5. The excitation function for the ratios (a) r_1, (b) r_2, and (c) R at back angles ($\geqslant 100°$) are shown versus the four-momentum transfer squared $-t$. Experimental data are from Refs. [1,2,6] and the present experiment (142-MeV data are shown by circles, 180-MeV data by diamonds, 220-MeV data by squares, and 256-MeV data by triangles).

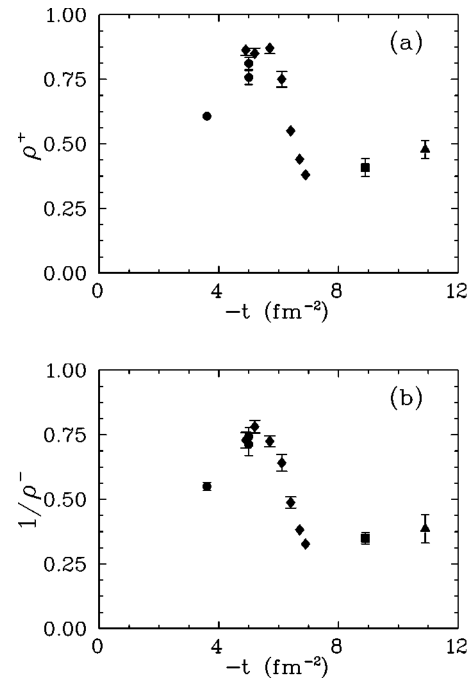

FIG. 6. The excitation function for the ratios (a) ρ^+ and (b) $1/\rho^-$ at back angles ($\geqslant 100°$) are shown versus the four-momentum transfer squared $-t$. The notation for the experimental data is the same as for Fig. 5.

tic π-^3A scattering quite nicely. However, for angles greater than 100°, we should consider two-step processes, especially double scattering, to explain π-^3A elastic scattering. All of the ratios are seen to be smooth functions of the momentum transfer, as can be inferred from the accompanying theory paper of Kudryavtsev *et al.* [7].

V. CONCLUSIONS

We present ten new measurements of the ratios r_1, r_2, and R at energies $T_\pi = 142$, 180, 220, and 256 MeV at backward scattering angles. These data complete and, where they overlap, are consistent with our data sets from previous measurements at smaller angles and the same energies [1–3,6]. At $T_\pi = 180$ MeV, the charge-symmetric ratios r_1, r_2, and R are smooth functions of the scattering angle in the backward hemisphere. The ratios r_1 and r_2 cross each other at around 120°; r_1 becomes significantly different from 1.00 at backward angles while r_2, which had been greater than 1.00 at forward angles, approaches unity. Deviation of the ratios r_1, r_2, and R from unity gives evidence for charge-symmetry-violation effects in these reactions. All three ratios, at energies of 180, 220, and 256 MeV, are well described by the theoretical approach of Ref. [7]. Additionally, the ratios at 180 MeV match well with the results of a previous calculation [10] that determines the value of the difference between the even and odd radii of ^{3}He and ^{3}H. It also has been shown that all three ratios r_1, r_2, and R (as well as ρ^+ and ρ^-) at scattering angles $\geqslant 100°$ and for all T_π studied can be described as a function of $-t$ only in the region where two-step processes, such as double scattering, dominate the π-^3A elastic scattering.

ACKNOWLEDGMENTS

The authors acknowledge the support of the U.S. National Science Foundation, the U.S. Department of Energy, the Croatian Ministry of Science, and the GW Research Enhancement Fund. We wish to thank R. Boudrie, C. Morris, and S. Dragic for their assistance during the running of the experiment and A. E. Kudryavtsev and I. I. Strakovsky for a careful reading of the manuscript and for fruitful discussions.

[1] B.M.K. Nefkens, W.J. Briscoe, A.D. Eichon, D.H. Fitzgerald, A. Mokhtari, J.A. Wightman, and M.E. Sadler, Phys. Rev. C **41**, 2770 (1990).

[2] C. Pillai, D.B. Barlow, B.L. Berman, W.J. Briscoe, A. Mokhtari, B.M.K. Nefkens, and M.E. Sadler, Phys. Rev. C **43**, 1838 (1991).

[3] W.J. Briscoe, B.L. Berman, R.W. Caress, K.S. Dhuga, S. Dragic, D. Knowles, D. Macek, S.K. Matthews, N.J. Nicholas, M.F. Taragin, D.B. Barlow, B.M.K. Nefkens, C. Pillai, J. Price, L.D. Isenhower, M.E. Sadler, S.J. Greene, I. Slaus, and I. Supek, Nucl. Phys. **A553**, 585 (1993).

[4] S.K. Matthews, W.J. Briscoe, C. Bennhold, B.L. Berman, R.W. Caress, K.S. Dhuga, S.N. Dragic, S.S. Kamalov, N.J. Nicholas, M.F. Taragin, L. Tiator, D.B. Barlow, B.M.K. Nefkens, C. Pillai, J.W. Price, L.D. Isenhower, M.E. Sadler, I. Šlaus, and I. Supek, Phys. Rev. C **51**, 2534 (1995); S. K. Matthews, Ph.D. thesis, The George Washington University, 1992.

[5] B.L. Berman, G.C. Anderson, W.J. Briscoe, A. Mokhtari, A.M. Petrov, M.E. Sadler, D.B. Barlow, B.M.K. Nefkens, and C. Pillai, Phys. Rev. C **51**, 1882 (1995).

[6] K.S. Dhuga, B.L. Berman, W.J. Briscoe, R.W. Caress, S.K. Matthews, D.B. Barlow, B.M.K. Nefkens, C. Pillai, J.W. Price, S.J. Greene, I. Slaus, and I. Supek, Phys. Rev. C **54**, 2823 (1996).

[7] A.E. Kudryavtsev, V.E. Tarasov, B.L. Berman, W.J. Briscoe, K.S. Dhuga, and I.I. Strakovsky, Phys. Rev. C **66**, 054007 (2002), following paper; nucl-th/0109074.

[8] Kr.T. Kim, Y.E. Kim, and R.H. Landau, Phys. Rev. C **36**, 2155 (1987); Y.E. Kim, M. Krell, and L. Tiator, Phys. Lett. B **172**, 287 (1986); Y.E. Kim, Phys. Rev. Lett. **53**, 1508 (1984).

[9] W.J. Briscoe and B.H. Silverman, Phys. Rev. C **39**, 282 (1987).

[10] W.R. Gibbs and B.F. Gibson, Phys. Rev. C **43**, 1012 (1991); (private communication).

[11] G.R. Smith, D.R. Gill, D. Ottewell, G.D. Wait, P. Walden, R.R. Johnson, R. Olszewski, R. Rui, M.E. Sevior, R.P. Trelle, J. Brack, J.J. Kraushaar, R.A. Ristinen, H. Chase, E.L. Mathie, V. Pafilis, R.B. Schubank, N.R. Stevenson, A. Rinat, and Y. Alexander, Phys. Rev. C **38**, 240 (1988).

[12] R.A. Arndt, I.I. Strakovsky, and R.L. Workman, Phys. Rev. C **50**, 1796 (1994).

[13] Particle Data Group, D.E. Groom, *et al.*, Eur. Phys. J. C **15**, 1 (2000); 2001 off-year partial update for 2002 edition available on the PDG site http://pdg.lbl.gov